Measurement of the two-photon correlation of synchrotron radiation in the VUV region by a delay-time modulation technique

Yasuhiro Takayama,[a]* Hidetsugu Shiozawa,[a] Tetsuo Yoshida,[a] Chol Lee,[a] Kenji Obu,[a] Hideo Otsubo,[a] Tsuneaki Miyahara,[a] Shigeru Yamamoto[b] and Masami Ando[b]

[a]*Department of Physics, Faculty of Science, Tokyo Metropolitan University, 1-1 Minami-ohsawa, Hachioji-shi, Tokyo 192-0397, Japan, and* [b]*Institute of Material Structure Science, High Energy Accelerator Research Organization, 1-1 Oho, Tsukuba-shi, Ibaraki 305-0801, Japan. E-mail: takayama@phys.metro-u.ac.jp*

The two-photon correlation (second-order coherence) of synchrotron radiation in the VUV region ($h\nu = 55$ eV) has been measured using a novel photon-counting method. A new technique has been developed to measure a small bunching effect by using a coincidence unit composed of a constant fraction discriminator, a time-to-amplitude converter (TAC), a single-channel analyzer (SCA) and two solid-state switches. The path of the circuit through which the stop signal for the TAC passes can be changed by a control voltage generated by a function generator, and the relative arrival time of two photons on condition that the output signal from the SCA appears is consequently changed. By modulating the arrival time and measuring the output rate from the SCA with a digital lock-in amplifier, an apparent bunching effect has been observed which is characteristic of the chaotic light. The electron-beam emittance in the horizontal direction was estimated as 39^{+13}_{-8} nm rad by this experiment, and the value was consistent with the designed value of 36 nm rad.

1. Introduction

In the last decade, third-generation synchrotron light sources such as the APS, ESRF and SPring-8 have been constructed to obtain high-brilliance X-rays. One of the most important characteristics of these light sources is the extremely small emittance of the electron beam in the storage ring. In theoretical studies of the electron-beam emittance it was pointed out that the brightness function, which is determined by the electron-beam emittance, and the first-order spatial coherence of synchrotron radiation have a close relationship with each other, and it was shown that the electron-beam emittance in the accelerator is directly estimated by measuring the first-order spatial coherence of the synchrotron radiation (Kim, 1986; Mitsuhashi, 1998; Takayama *et al.*, 1998*b*; Takayama & Kamada, 1999). The experimental measurement of the emittance using synchrotron radiation has been developed and has proved to be an excellent technique, since the measurement does not disturb the electron beam in the storage ring. Moreover, it has been reported that the first-order spatial coherence of synchrotron radiation plays an important role in some experiments, such as imaging, X-ray absorption, speckle pattern and so on (Kirz *et al.*, 1992; Sutton *et al.*, 1991; Hunter Dunn *et al.*, 2000). For these reasons, some experiments for the direct measurement of the first-order spatial coherence have been performed in the visible, VUV, soft X-ray and hard X-ray regions (Baron *et al.*, 1996; Mitsu-

hashi, 1998; Takayama *et al.*, 1998*a*; Chang *et al.*, 2000; Kohn *et al.*, 2000; Paterson *et al.*, 2001).

Since the importance of the second-order coherence of synchrotron radiation was discussed about ten years ago (Ikonen, 1992), several attempts to measure the second-order coherence have also been performed (Gluskin *et al.*, 1994, 1999; Kunimune *et al.*, 1997; Tai *et al.*, 1999; Yabashi *et al.*, 2001). As the photon statistics can be investigated by measuring the second-order coherence, we can distinguish whether the light is coherent, chaotic or squeezed. Therefore, the characteristics of the FEL or SASE whose photon statistics are different from the usual synchrotron radiation (chaotic light) will be investigated. On the other hand, if the photon statistics are known to be chaotic, the first-order coherence can be estimated from the second-order coherence (Mandel & Wolf, 1995). Generally, it is very difficult to perform an accurate measurement of the second-order coherence because the temporal coherence of X-rays is much shorter than the response time of the electric circuit and the bunching effect is smoothed by the long response time. An exception is the recent experiment performed by Yabashi *et al.* (2001). In their experiment the bandwidth of the monochromator was only 120 µeV which corresponded to 30 ps temporal coherence, and a clear bunching effect was observed with high accuracy. In the VUV and soft X-ray regions, on the other hand, the light is monochromated by a grating monochromator, and light with such a long temporal coherence cannot be obtained. To overcome the problem in these energy regions, Tai *et al.* (1999) developed a novel technique of measuring a small bunching effect with a lock-in amplifier. They modulated the width of the entrance slit of the monochromator to modulate the temporal coherence. The third-harmonic component of the modulation frequency in the signal, which contains information on the second-order coherence, was measured with a lock-in amplifier. A serious problem in their measurement was that the non-harmonic motion of the modulation of the entrance slit gave a large error in the result.

The purpose of this study is to establish a novel technique to measure the second-order coherence by using an ordinary monochromator with an energy resolution $E/\Delta E$ of less than 10 000. For this purpose we modulated the relative arrival time of two photons and measured the first harmonic of the output of the coincidence rate. We explain the principle of the measurement in detail and report the first result of the experiment.

2. Experimental set-up

The experiment was performed at the undulator beamline BL-16B of the Photon Factory, KEK. The electron-beam energy in the storage ring was 2.5 GeV and the designed emittance of the electron beam in the horizontal direction was 36 nm rad. The circumference of the ring was 187 m and the revolution period was 624 ns. A basic diagram of the optical system of our instruments is shown in Fig. 1. Details of the system have been given elsewhere (Tai *et al.*, 2000). The light from the
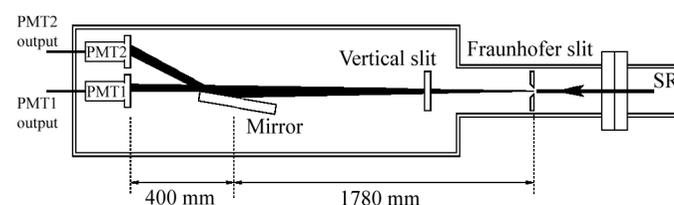
Figure 1
Top view of the optical system of the intensity interferometer.
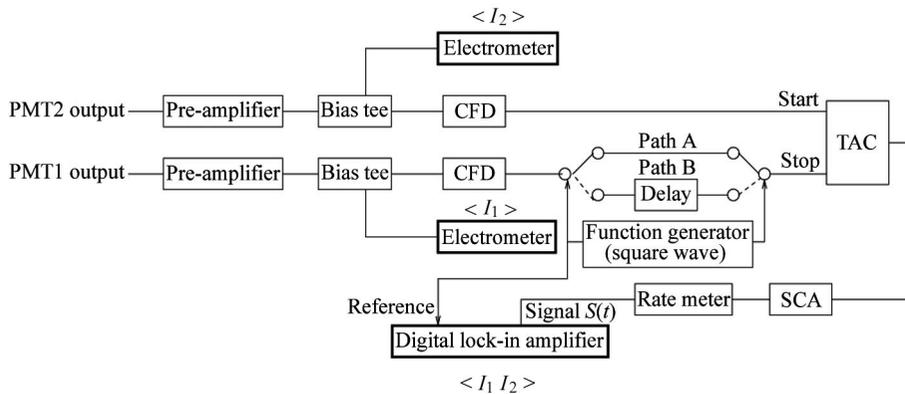
Figure 2
High-frequency circuit for measuring the correlation.

storage ring was monochromated by a dragon-type monochromator (Shigemasa *et al.*, 1998). The photon energy of the monochromated light was 55 eV and the energy resolution $E/\Delta E$ was ∼5000. The monochromated light was diffracted by a Fraunhofer slit. The width of the slit was changed with an accuracy of 1 μm and the spatial coherence in the horizontal direction could be controlled by changing the width. The beam size on the slit, which is necessary to estimate the emittance, was measured using a tungsten wire scanner of thickness 50 μm. The spatial resolution of the wire, which is defined in this paper as the standard derivation of the sensitivity function of the wire, is 14.4 μm (= $50.0/\sqrt{12}$ μm) by approximating the sensitivity function with a Gaussian shape. A mirror divides the beam into two parts and each part was measured using a photomultiplier tube (PMT; Hamamatsu R5150). In order to keep the intensity of the beam at the PMTs constant under different conditions of the Fraunhofer slit, we adjusted the vertical slit that is located between the Fraunhofer slit and mirror. This vertical slit did not change the spatial coherence, because the spatial coherence in the vertical direction was almost perfect at the photon energy of 55 eV, which had been verified in the measurement of the first-order coherence with a Young's interferometer (Takayama *et al.*, 1998a). Moreover, the light passes through a beamline monochromator which contains entrance and exit slits with fixed widths of 25 μm, and the vertical coherence will be improved further before the light enters the vertical slit. For these reasons the vertical slit after the Fraunhofer slit will not improve the spatial coherence any further.

The outputs of the two PMTs were analyzed by a set of high-frequency circuits as shown in Fig. 2. Each signal was divided into an RF signal and a DC signal by a bias tee. DC signals I_1 and I_2 were measured using two digital electrometers and were used to normalize the correlation. The gain of the PMT was about 10^6–10^7, and I_1 and I_2 were kept to ∼1 μA. Hence, the count rate of the photons detected by the PMT was expected to be about 10^6–10^7 counts s^{-1}. Each RF signal was amplified by a pre-amplifier (ORTEC 9306) and the pulse shape was formed by a constant fraction discriminator (CFD; OXFORD TC454). One of the outputs from the CFDs directly becomes the start input of a time-to-amplitude converter (TAC; ORTEC 457) and the other output becomes the stop input of the TAC. There are two paths between the CFD and the stop input of the TAC, and the path can be changed by two solid-state switches. One of the paths (B) has a delay relative to the other path (A). The stop signal to the TAC goes through path A or path B by applying a voltage of +10.2 or −10.2 V to the control input of the solid-state switches, respectively. We adjusted the delay to be 624 ns which

corresponded to the revolution period of the electron beam in the storage ring as shown in Fig. 3. The output of the TAC passes into a single-channel analyzer (SCA) and the pulse with a selected height is discriminated. Consequently, a signal appears from the SCA only when the start and stop signals come into the TAC with a definite delay. In our experiment the cable length was adjusted as a signal from the SCA appeared when two photons simultaneously appeared at the PMTs and the stop signal of the TAC went through path A. Therefore, the correlation of the two photons emitted from one bunch is taken when a voltage of +10.2 V is applied to the switches (path A), and the correlation of two photons emitted from a bunch and the bunch which has undergone one lap of a storage ring is taken when a voltage of −10.2 V is applied to the switches (path B). If the subtraction of the correlation for two arrangements is measured, the correlation due to the bunch structure of the electron beam, which we call the trivial correlation, is minimized, and the correlation due to the chaotic nature is clearly observed. For this purpose the output rate of the SCA was measured using a ratemeter (ORTEC 449) and the analog output of the ratemeter passed into a digital lock-in amplifier (SRS 830). The input rate of the TAC was about 10^5–10^6 counts s^{-1} and the output rate of the SCA, which corresponded to the coincidence rate including the trivial correlation, was about 10–50 counts s^{-1}. The reference signal of the lock-in amplifier was generated by a function generator, and the waveform of the reference signal was a square wave whose amplitude, offset and frequency were 10.2 V, 0 V and 0.795 Hz, respectively. The reference signal was also used as a control input for the solid-state switches.

The output of the digital lock-in amplifier is a two-dimensional vector $\mathbf{W} = (W_x, W_y)$ which is defined as

$$W_x + iW_y = (1/T) \int\limits_t^{t+T} dt'\, S(t') \exp(i\omega_{\mathrm{ref}} t'), \qquad (1)$$

where $S(t')$ is the input signal of the lock-in amplifier and ω_{ref} is the angular frequency of the reference signal. T is the time constant of the lock-in amplifier and is much larger than $2\pi/\omega_{\mathrm{ref}}$. The signal from the digital lock-in amplifier $\mathbf{W}$, and DC signals I_1 and I_2 were transferred to a computer every second and the signals were averaged.

3. Method of theoretical analysis

In order to derive the analytic form for $\mathbf{W}$ in equation (1), we make a simplified model calculation as shown in Fig. 4. $E(x, 0)$ and $E(x, L)$ denote the electric fields on the Fraunhofer slit and the detectors, respectively, where L is the distance between the Fraunhofer slit and
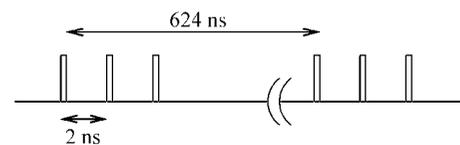
Figure 3
Time structure of the synchrotron radiation of the Photon Factory ring. The interval between the bunches is 2 ns and the revolution period is 624 ns. The bunches are partially filled.

the detectors. If the beam on the Fraunhofer slit is supposed to be a Gaussian beam, the beam profile on the Fraunhofer slit $I(x)$ is given by

$$I(x) \equiv \langle |E(x, 0)|^2 \rangle = I(0) \exp\left(-x^2/2\Sigma^2\right), \qquad (2)$$

where Σ is the beam size on the Fraunhofer slit and is measured using a wire scanner. The first-order spatial coherence on the Fraunhofer slit $\gamma^{(1)}(d)$ is given by (Takayama *et al.*, 1998b)

$$\gamma^{(1)}(d) \equiv \frac{\langle E^*(d/2, 0)E(-d/2, 0) \rangle}{\left[\langle |E(d/2, 0)|^2 \rangle \langle |E(-d/2, 0)|^2 \rangle \right]^{1/2}}$$
$$= \exp\left(-d^2/8\sigma_c^2\right), \qquad (3)$$

where σ_c is the spatial coherent size on the Fraunhofer slit defined as

$$\sigma_c = \varepsilon_p \Sigma / \left(\varepsilon^2 - \varepsilon_p^2\right)^{1/2}, \qquad (4)$$

$$\varepsilon_p = \lambda/4\pi. \qquad (5)$$

λ is the wavelength of the photon and ε is the total photon emittance which is a convolution of the contributions from the electron beam and one-photon beam. ε_p is the one-photon emittance and takes a value of 1.79 nm rad for a photon energy of 55 eV. The probability of the coincidence rate $P(D)$ is given by the integral of the product of the intensities of the lights on two detectors. Since the beam size on the detector is much smaller than the active area of the detector, the integral area is approximately extended as follows,
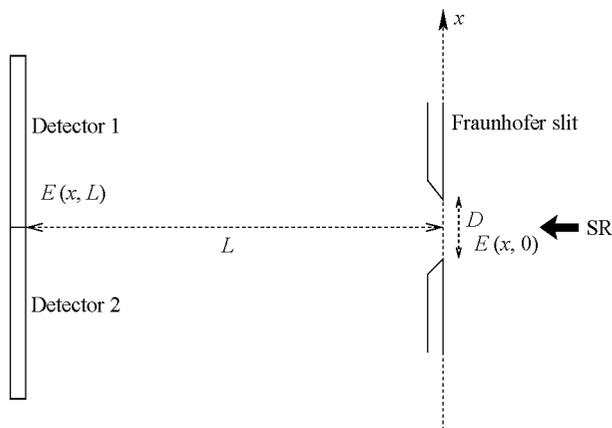
$$P(D) \propto \int\limits_0^\infty \mathrm{d}x_1 \int\limits_{-\infty}^0 \mathrm{d}x_2 \langle |E(x_1, L)|^2 |E(x_2, L)|^2 \rangle$$
$$= I_1 I_2 G(D) + I_1 I_2, \qquad (6)$$

where the light is assumed to be chaotic and stationary, and

$$G(D) = (1/I_1 I_2) \int\limits_0^\infty \mathrm{d}x_1 \int\limits_{-\infty}^0 \mathrm{d}x_2 \left| \langle E^*(x_1, L)E(x_2, L) \rangle \right|^2, \qquad (7)$$

$$I_1 = \int\limits_0^\infty \mathrm{d}x_1 \langle |E(x_1, L)|^2 \rangle, \qquad (8)$$

$$I_2 = \int\limits_{-\infty}^0 \mathrm{d}x_2 \langle |E(x_2, L)|^2 \rangle. \qquad (9)$$

Figure 4
Arrangement of the Fraunhofer slit and the detectors for the calculation of the two-photon correlation.

I_1 and I_2 are the intensities of the lights on detectors 1 and 2, respectively. The first term in (6) is characteristic of the chaotic light and this does not exist for coherent light. The second term in (6) is known as an accidental coincidence. The electric field on the detector is calculated using the electric field on the Fraunhofer slit and the transmittance function of the Fraunhofer slit $T(x)$ as follows,

$$E(x, L) \simeq [\exp(ikL)/L] \int \mathrm{d}x' \, T(x')E(x', 0) \exp\left\{ [ik(x - x')^2]/2L \right\}, \qquad (10)$$

where $k = 2\pi/\lambda$ is the wavenumber. The transmittance function should be

$$T(x) = \begin{cases} 1/D & |x| \le D/2 \\ 0 & |x| > D/2 \end{cases}. \qquad (11)$$

However, this function is not appropriate for analytical calculation and we approximate the function with a Gaussian transmittance function,

$$T(x) = \left(2\pi D/12^{1/2}\right)^{-1/2} \exp\left(-6x^2/D^2\right). \qquad (12)$$

It is noted that the two transmittance functions in (11) and (12) give the same second moment $\langle x^2 \rangle = D^2/12$. By substituting (10) and (12) into (7), $G(D)$ is represented by the correlation function on the double slit $\langle E^*(x_1, 0)E(x_2, 0) \rangle$ whose analytical form has been obtained by using the Gaussian beam approximation (Takayama *et al.*, 1998b). A somewhat complicated calculation gives the following result,

$$G(D) = \frac{2}{\pi} \left[\frac{D^2 + 24\Sigma^2}{(1 + \Sigma^2/\sigma_c^2)D^2 + 24\Sigma^2} \right]$$
$$\times \cos^{-1}\left[\frac{D^2}{(1 + 2\sigma_c^2/\Sigma^2)D^2 + 48\sigma_c^2} \right]. \qquad (13)$$

For a stationary light, the output of the SCA $S(t)$ is proportional to $P(D)$ defined in (6) and we have

$$S(t) = \alpha P(D) = \alpha I_1 I_2 G(D) + \alpha I_1 I_2, \qquad (14)$$

where α is a positive constant. The electron beam in the storage ring forms the bunch structure and is not regarded as a stationary light source. This gives another contribution to $S(t)$ as follows,

$$S(t) = \alpha I_1 I_2 G(D) + \alpha I_1 I_2 + \alpha I_1 I_2 A. \qquad (15)$$

A is a trivial correlation determined by the form of the bunch. If we modulate the paths between A and B, $G(D)$ and A should be modified as follows,

$$G(D) \rightarrow G(D)f(t + t'), \qquad (16)$$

$$A \rightarrow A f(t + t'), \qquad (17)$$

where $f(t)$ is proportional to the control voltage generated by the function generator and t' is determined by the phase relation between the control voltage and the signal. In our experiment, t' should be zero, because the coincidence rate should increase (decrease) when the control voltage applied to the solid-state switch is +10.2 V (-10.2 V) and the phase of the control voltage and the signal of the correlation should be equal as shown in Fig. 5. The second term in equation (15) has no time dependence since it is the accidental coincidence. By substituting (15), (16) and (17) into (1), we have

$$\langle \mathbf{W} \rangle / I_1 I_2 \equiv \mathbf{V} = \beta G(D)\mathbf{s} + \beta A\mathbf{s}, \qquad (18)$$

where $\mathbf{s}$ is a unit vector defined as $(1, 0)$ and β is a positive constant. The second term in (18) comes from the bunch structure of the electron beam and is ideally zero by modulating the paths between A
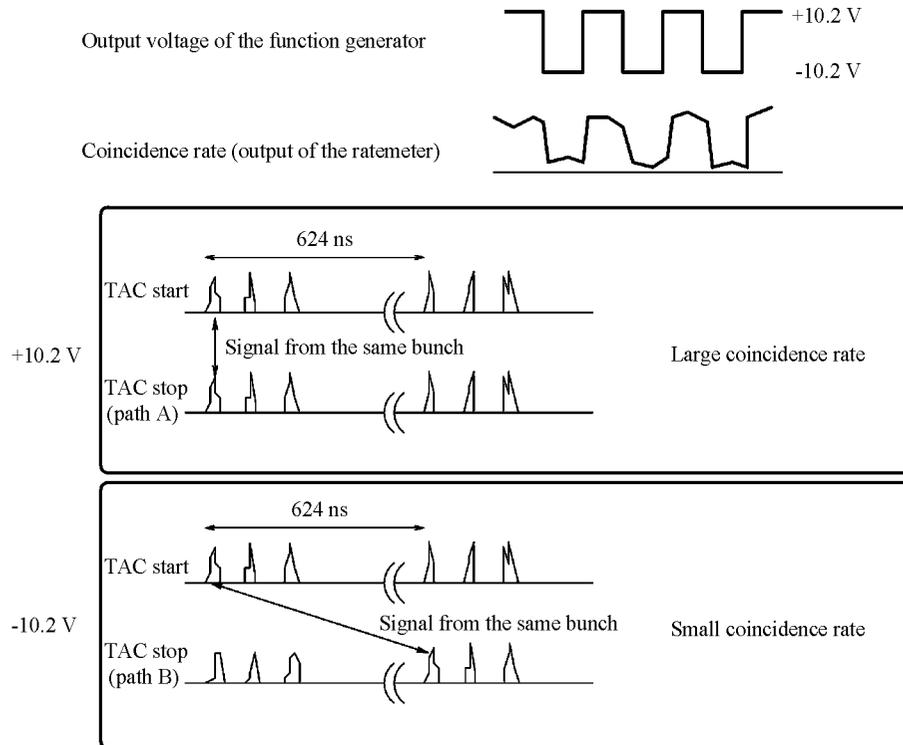
Figure 5
Timing of applying the control voltage to the solid-state switches and the output of the ratemeter. When +10.2 V (−10.2 V) is applied to the switches, the coincidence of the two photons emitted from the same (different) bunch is taken, and the coincidence rate increases (decreases). Consequently, the phase difference between the control voltage generated by the function generator and the output of the SCA is zero.
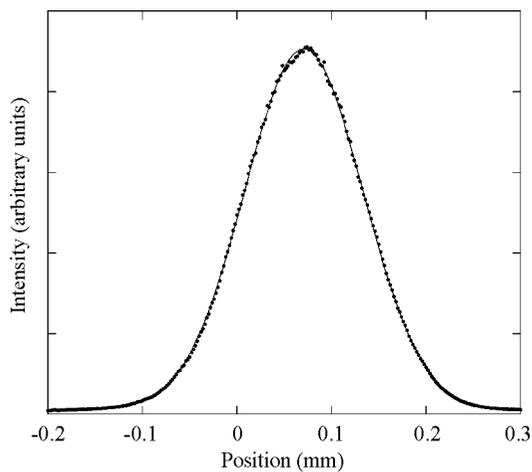
Figure 6
Beam profile on the Fraunhofer slit measured using a tungsten wire scanner. The standard derivation is estimated to be 62.6 µm.

and B, since the correlation due to the bunch structure does not depend on which path the signal has gone through if the delay is precisely adjusted to be 624 ns. However, we kept the term considering some errors, such as the incomplete adjustments of the delay, in the experiment. From (13) and (18) we find that **V** should move towards the direction of **s** as D decreases, since $G(D)$ is a decreasing function for $D \geq 0$.

Only the x component in (18) has significant information on the spatial coherence and is written as

$$V_x = \beta G(D) + \beta A. \tag{19}$$

By fitting the obtained V_x with (13) and (19) we can estimate the spatial coherent size σ_c, and the total photon emittance ε can be estimated with the help of (4) and (5).

4. Result and discussions

The beam profile on the Fraunhofer slit measured using the wire scanner is shown in Fig. 6. The standard deviation of the beam profile is 62.6 µm, and the beam size Σ defined in (2) is estimated to be 60.9 µm by subtracting the contribution of the spatial resolution of the tungsten wire, 14.4 µm.

For the measurement of the two-photon correlation we have changed the width of the Fraunhofer slit D for several conditions between 8 µm and 96 µm. For each measurement we accumulated the data for ∼5–6 h. Fig. 7 shows the plots of **V** in (19) for each D. The numbers in the figure denote the width of the Fraunhofer slit D. The error bars in the figure come from the statistical error due to the large fluctuation of the output of the lock-in amplifier. The points tend to move towards the direction of **s** = (1, 0) as the width of the Fraunhofer slit becomes narrower, which is expected from the theoretical calculation in the previous section. Although all points should lie on a line V_y = constant, the points for $D = 20$ and 64 µm are off the line beyond the statistical error. However, the total shift of the points due to the change of D is much larger than this error. We later discuss the origin of the error. Fig. 8 shows a plot of V_x as a function of D. The best-fitted curve using (13) and (19) is also shown in the figure. V_x tends to decrease as D is increased, which is known as the bunching effect of chaotic light. Thus, this result clearly shows that the

synchrotron radiation has a chaotic component. From the fitted curves the spatial coherent size σ_c was estimated as 2.9 µm, and the total photon emittance ε was calculated as 39^{+13}_{-8} nm rad. The designed value of the electron-beam emittance in the horizontal direction of the Photon Factory is 36 nm rad, and this value is much larger than the intrinsic photon emittance, 1.79 nm rad, for a photon energy of 55 eV. Therefore, the total photon emittance is approximately the same as the electron-beam emittance, and our experiment gives a reasonable value of the electron-beam emittance.

In Fig. 8, V_x seems to converge to negative values in the limit $D \to \infty$. Since $G(D)$ in (13) is positive definite, this result shows that A in (18) and (19) determined by the bunch structure of the electron beam must be a negative value. If the adjustment of the delay in the circuit is complete, the trivial correlation is cancelled out by the modulation and A must be zero. The negative value of A means that the correlation with the path B is stronger than that with the path A, but this may not be explained by assuming the incomplete adjustment of the delay module, since the adjustments of the cable length for path A is much easier than that for path B. The solid-state switch has a power loss of about 3 dB and some pulses were lost at the switches. If the power losses at the switches in paths A and B were not equal and more pulses were lost in the path A, A may become negative. It is noted that this problem only has an influence on A and no correction is necessary for $G(D)$. The reason for the discrepancy concerning V_y for $D = 20$ µm and 64 µm in Fig. 7 is not clear at present, but we discuss some possible sources which may cause some errors in our experiment. First, the dead time of the high-frequency circuit may break the simple relation in (18). We have measured I_1 and I_2 as the electric currents which should not be affected by the dead time of the circuit and detector. $\mathbf{W}$, on the other hand, is very sensitive to the dead time, since $\mathbf{W}$ is measured after the signal is transferred to the pulse in the circuit. If the input rates for both the start and stop inputs of the TAC are f Hz and the window width of the output is τ s, the output rate of the SCA $R(f)$ is given by τf^2 Hz. The definition of τ is that a signal appears from the SCA when two photons appear at two detectors within the interval of τ. In our experiments, τ was adjusted to be a fixed value of 1 ns. Fig. 9 shows a comparison of the experi-

mental result and the theoretical calculation for $R(f)$ as a function of f. For small f less than 100 kHz, the experimental result is almost consistent with the theoretical curve. However, as the frequency becomes larger the discrepancy between the two results becomes clear, and this is caused by the dead time of the high-frequency circuit, such as the CFD, TAC and delay module. Including the effect of the dead time T_d, $R(f)$ is modified as

$$R(f) = \tau\left[f/(1 + f\, T_d)\right]^2. \tag{20}$$

The experimental result fits well to this equation and the dead time T_d is estimated to be 1.62 µs as shown in Fig. 9. Then we inevitably modify the definition of $\mathbf{V}$ in (18) as

$$\mathbf{V} \equiv \langle\mathbf{W}\rangle / \left\{\left[I_1/(1 + I_1\hat{T}_d)\right]\left[I_2/(1 + I_2\hat{T}_d)\right]\right\}, \tag{21}$$

where $\hat{T}_d$ is a parameter of the saturation due to the dead time. Unfortunately we did not count the input rate but instead measured
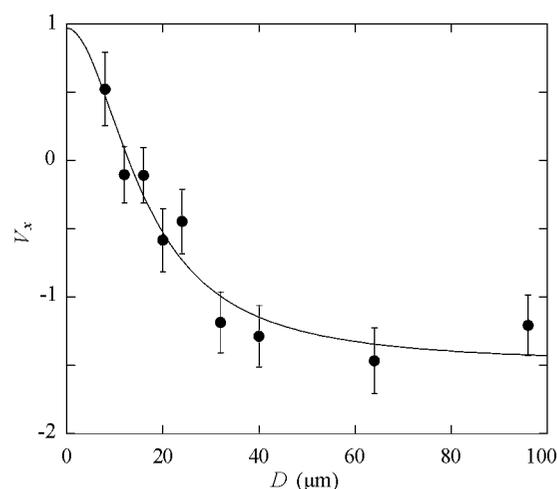
Figure 8
Plot of V_x as a function of the width of the Fraunhofer slit D. The curve is the best-fitted curve defined in equation (19).
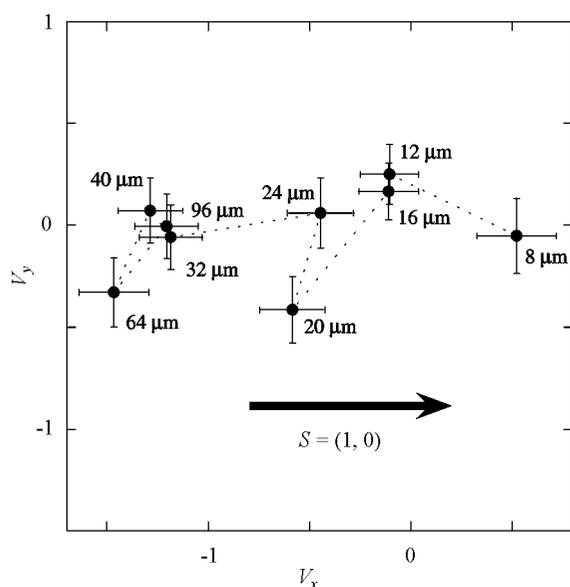
Figure 7
Plot of $\mathbf{V}$ for each Fraunhofer slit width D. The arrow in the figure indicates the direction of $\mathbf{s}$. As the width of the slit becomes narrower, the points tend to move towards the direction of $\mathbf{s} = (1, 0)$.
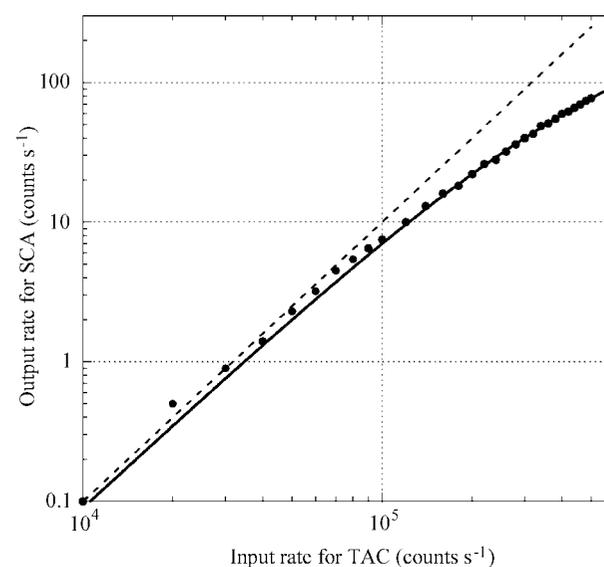
Figure 9
Output rate for SCA as a function of the input rate for the TAC. The input rate for start and stop inputs of the TAC was adjusted to be equal. The solid line is the best-fitted curve defined in equation (20) and the dashed line is the expected curve without the dead time.

Yasuhiro Takayama *et al.* • Two-photon correlation measurement   **307**

the input rate as an electric current which was proportional to the actual count rate without the effect of the dead time. We cannot know the correct value of $\hat{T}_d$, but we have confirmed that $\mathbf{V}$ in (21) was almost independent of $\hat{T}_d$. Therefore, we conclude that the systematic error due to the dead time is not important in this measurement. Another possible error might occur in the optical set-up or electric circuits. When we changed the width of the Fraunhofer slit we only adjusted the width of the vertical slit and the position of the mirror for splitting the beam, but we did not change any parameters of other optical elements and electric circuits. If the center of the Fraunhofer slit or vertical slit was shifted to the edge of the beam, the degree of the spatial coherence might decrease. However, this error does not influence V_y but rather V_x. As a result, we conclude that the most probable origin of the error is noise in the electric circuits. Although we did not change the parameters of the electric circuits, some small systematic noise may be introduced into the lock-in amplifier in some measurements owing to changes in the conditions in the laboratory.

We also need to discuss the justification of the approximations in the theoretical calculation. To derive equation (13) we applied two daring approximations: that the synchrotron radiation was assumed to be a Gaussian beam and that the transmittance function of the Fraunhofer slit was assumed to have a Gaussian shape. We have already shown that the Gaussian beam approximation for the undulator radiation is not applicable unless certain conditions are satisfied (Takayama *et al.*, 2000). The approximation for the transmittance function of the Fraunhofer slit may not be appropriate either, since the diffraction patterns of the Gaussian slit and the actual slit are quite different from each other. At present, we have tentatively used them in order to obtain the analytical function. To derive more reliable values of the electron-beam emittance from the experimental data, we need to perform the numerical calculations described by Takayama *et al.* (2000).

We have shown that the electron-beam emittance could be estimated by measuring the first-order spatial coherence with a Young's interferometer. The interference pattern in the VUV region was measured using a photomultiplier by scanning it on the one-dimensional axis with a 5 µm resolution (Takayama *et. al.*, 1998*a*). It took about 30 min to measure an interference pattern, which is much shorter than the accumulation time in the experiment of the second-order coherence explained in this paper. Moreover, the measurement using a Young's interferometer directly gives the first-order spatial coherence and the theoretical treatment is much easier than the calculation in this paper. One may doubt the merit of measuring the second-order coherence rather than the first-order coherence for the estimation of the electron-beam emittance. For the measurement of an interference pattern with a Young's interferometer, we need to accumulate the photons for at least several milliseconds, even if we use a two-dimensional detector, such as a CCD camera. If the orbit of the electron beam is distorted during the measurement, the electron-beam emittance will be estimated as a larger value compared with the designed value. On the other hand, the instability of the electron beam which is slower than the temporal coherence (~ 1 ps) does not affect the two-photon correlation. For the same reason, an intensity interferometer instead of a Michelson interferometer, which is seriously affected by the fluctuation of the atmosphere, was constructed to measure the apparent diameter of the star (Hanbury Brown, 1974).

In order to improve the measurement of the two-photon correlation as a useful tool for the diagnosis of the electron and photon beams, we need to shorten the accumulation time. Unfortunately, the technique explained in this paper has a limitation due to the dead

time. The accumulation time in this measurement is determined by the output rate of the SCA. According to equation (20), the output rate is limited to $\tau/T_d^2 \simeq 400$ counts s^{-1} owing to the dead time. Therefore, even if we can use extremely bright synchrotron radiation, we need to accumulate for about 1 h to achieve an acceptable signal-to-noise ratio. This is certainly a problem for any technique where the two-photon correlation is measured by electric circuits with a long dead time. If the two-photon correlation is measured using a non-linear optics technique, this problem will hopefully be solved. For example, the probability of the two-photon core absorption is proportional to the second-order coherence, and the lifetime of the intermediate state corresponds to the dead time of our measurement (Teicht & Wolga, 1966). The lifetime for the core absorption in the soft X-ray region is expected to be less than 10^{-14} s. This technique is a promising candidate for measuring the higher-order coherence for extremely intense X-rays, such as the SASE.

In summary, we have succeeded in an accurate measurement of the two-photon correlation by modulating the timing of the coincidence. A bunching effect was clearly observed even though the energy resolution of the monochromator was not extremely high. Therefore, this technique will also be applicable in the soft X-ray region. We have also succeeded in deriving a consistent value for the electron-beam emittance from the measurement. The improvement of the signal-to-noise ratio in the experiment and the more accurate methods for the theoretical calculation are required, which will be solved in future works.

References

Baron, A. Q. R., Chumakov, A. I., Grünsteudel, H. F., Grünsteudel, H., Nielsen, L. & Rüffer, R. (1996). *Phys. Rev. Lett.* **77**, 4808–4811.

Chang, C., Naulleau, P., Anderson, E. & Attwood, D. (2000). *Opt. Commun.* **182**, 25–34.

Gluskin, E., Alp, E. E., McNulty, I., Sturhahn, W. & Sutter, J. (1999). *J. Synchrotron Rad.* **6**, 1065–1066.

Gluskin, E., McNulty, I., Yang, L., Randall, K. J., Xu, Z. & Johnson, E. D. (1994). *Nucl. Instrum. Methods*, A**347**, 177–181.

Hanbury Brown, R. (1974). *The Intensity Interferometer.* London: Taylor & Francis.

Hunter Dunn, J., Arvanitis, D., Carr, R. & Mårtensson, N. (2000). *Phys. Rev. Lett.* **84**, 1031–1034.

Ikonen, E. (1992). *Phys. Rev. Lett.* **68**, 2759–2761.

Kim, K.-J. (1986). *Nucl. Instrum. Methods*, A**246**, 71–76.

Kirz, J., Abe, H., Jacobsen, C., Ko, C.-H., Lindaas, S., McNulty, I., Sayre, D., Williams, S., Zhang, X. & Howells, M. (1992). *Rev. Sci. Instrum.* **63**, 557–563.

Kohn, V., Snigireva, I. & Snigirev, A. (2000). *Phys. Rev. Lett.* **85**, 2745–2748.

Kunimune, Y., Yoda, Y., Izumi, K., Yabashi, M., Zhang, X.-W., Harami, T., Ando, M. & Kikuta, S. (1997). *J. Synchrotron Rad.* **4**, 199–203.

Mandel, L. & Wolf, E. (1995). *Optical Coherence and Quantum Optics.* Cambridge University Press.

Mitsuhashi, T. (1998). *Proceedings of the 1997 Particle Accelerator Conference*, Vol. 1, pp. 766–768. Piscataway, NJ: IEEE.

Paterson, D., Allman, B. E., MacMahon, P. J., Lin, J., Moldovan, N., Nugent, K. A., McNulty, I., Chantler, C. T., Retsch, C. C., Irving, T. H. K. & Mancini, D. C. (2001). *Opt. Commun.* **195**, 79–84.

Shigemasa, E., Toyoshima, A., Yan, Y., Hayaishi, T., Soejima, K., Kiyokura, T. & Yagishita, A. (1998). *J. Synchrotron Rad.* **5**, 777–779.

Sutton, M., Mochrie, S. G. J., Greytak, T., Nagler, S. E., Bergman, L. E., Held, G. A. & Stephenson, G. B. (1991). *Nature (London)*, **352**, 608–610.

Tai, R. Z., Takayama, Y., Takaya, N., Miyahara, T., Yamamoto, S., Sugiyama, H., Urakawa, J., Hayano, H. & Ando, M. (1999). *Phys. Rev. A*, **60**, 3262–3266.

Tai, R. Z., Takayama, Y., Takaya, N., Miyahara, T., Yamamoto, S., Sugiyama, H., Urakawa, J., Hayano, H. & Ando, M. (2000). *Rev. Sci. Instrum.* **71**, 1256–1263.

Takayama, Y., Hatano, T., Miyahara, T. & Okamoto, W. (1998*b*). *J. Synchrotron Rad.* **5**, 1187–1194.

Takayama, Y. & Kamada, S. (1999). *Phys. Rev. E*, **59**, 7128–7140.

Takayama, Y., Shiozawa, H., Takaya, N., Miyahara, T. & Tai, R. Z. (2000). *Nucl. Instrum. Methods*, A**455**, 217–221.

Takayama, Y., Tai, R. Z., Hatano, H., Miyahara, T., Okamoto, W. & Kagoshima, Y. (1998*a*). *J. Synchrotron Rad.* **5**, 456–458.

Teicht, M. C. & Wolga, G. J. (1966). *Phys. Rev. Lett.* **16**, 625–628.

Yabashi, M., Tamasaku, K. & Ishikawa, T. (2001). *Phys. Rev. Lett.* **87**, 140801-1–140801-4.

309